Kardiologia Polska 2012; 70, 10: 989–997 ISSN 0022–9032

ORIGINAL ARTICLE

The determinants of side branch compromise after main vessel stenting in coronary bifurcation lesions

Dobrin Vassilev[1], Robert J. Gil[2, 3], Bon-Kwon Koo[4], C. Michael Gibson[5], Thach Nguyen[6], Thai Hoang[7], Nina Gotcheva[8]

[1]Cardiac Catheterisation Laboratory, National Heart Hospital, Sofia, Bulgaria; [2]Invasive Cardiology Clinic, Central Clinical Hospital of the Internal Affairs and Administration Ministry, Warsaw, Poland; [3]Institute of Experimental and Clinical Medicine, Polish Academy of Science, Warsaw, Poland; [4]Seoul National University Hospital, South Korea; [5]Cardiovascular Division, Beth Israel Deaconess Medical Center, Harvard Medical School, Boston, MA, USA; [6]St. Mary Medical Center, Hobart, IN, USA; [7]University of Arizona, Sarver Heart Center, Southern Arizona VA Health Care System, Tucson, AZ, USA; [8]National Heart Hospital, Sofia, Bulgaria

Abstract

Background and aim: The purpose of this analysis was to determine the factors responsible for side branch (SB) ostial stenosis after main vessel stent implantation.

Methods: Theoretical and bench-test bifurcation models with different lengths of carina were created. Bench-test experiments with a flexible bifurcation model were performed for the observation of changes in the bifurcation region after stent implantation. An angiographic analysis of 92 bifurcation lesions (84 patients) was performed to determine the role of theoretical parameters on SB compromise in practice. The theoretically predicted and actual SB compromise were compared in these patients.

Results: Bench tests revealed a complex change in the bifurcation region with carina displacement, SB lateral walls stretch and main vessel — SB proximal angle decrease after main vessel stent placement. In an angiographic analysis, actually measured SB% diameter stenosis was larger than expected in 35 (38%) lesions and the measured stenosis was smaller than expected in 49 lesions. Independent predictors of difference between theoretically predicted and observed SB stenosis were carina length mismatch (OR = 2.568, CI 1.336–4.896), main branch reference diameter (OR = 0.314, CI 0.101–0.972), and proximal main vessel — SB angle change after stenting (OR = 0.926, CI 0.870–0.985). In a plot comparing the values of carina length mismatch and deviations from the prediction in SB ostial stenosis, 30% (n = 27) of cases were located in a zone with a shorter carina and more SB compromise than expected, suggesting the role of plaque shift in these cases.

Conclusions: The degree of SB jailing seems to be determined by carina deformation, the length of the carina, and plaque shifting.

Key words: coronary bifurcation stenting, carina deformation, carina length, plaque shift

Kardiol Pol 2012; 70, 10: 989–997

INTRODUCTION

Bifurcation lesions still pose a treatment problem due to a higher rate of periprocedural myocardial infarction and long term restenosis [1–6]. A recent report suggested that there may be a direct relation between the degree of side branch (SB) ostial stenosis and the appearance of myonecrosis on magnetic resonance delayed gadolinium enhancement images [7]. Moreover, as some patients still need two stents during the provisional strategy, it would be more helpful to the operators if those patients who will have severe stenosis after main branch (MB) stenting could be predicted before the procedure. The mechanism of SB jailing is complex. Our group proposed and verified the importance of carina relocation [8–11] and a recent study suggested that SB jailing is caused

Address for correspondence:
Dobrin Vassilev, MD, PhD, Cardiac Catheterisation Laboratory, National Heart Hospital, Sofia, Bulgaria, 65 Koniovitza Str., 1309 Sofia, Bulgaria, e-mail: dobrinv@gmail.com

Received: 01.02.2012 **Accepted:** 09.05.2012

by both the plaque and carina shifts [12]. However, detailed analysis on the components of SB jailing has yet to be properly evaluated.

The purpose of the present analysis was to determine the factors responsible for SB jailing and for the deviation from the theoretical prediction of the degree of SB ostial stenosis after MB stent implantation. We established new theoretical bifurcation models, performed bench tests and applied theoretical concepts to patients with bifurcation lesions. This is an extension of our previous work on factors governing SB compromise and influencing carina displacement [8–11, 13].

METHODS

Theoretical models

A theoretical descriptive model for coronary bifurcation construction is presented in Appendix 1. This model permits analysis of the effects of the changes in different bifurcation parameters (branch diameters, vessel angulations) on the bifurcation confluence region (region of the connection of parent vessel [MV], main branch [MB] and side branch [SB]). The carina is a part of the bifurcation confluence region formed from the connection of SB and MB walls facing together. Thus, the carina has two walls, one from the MB and the other from the SB, with an angle formed between those two walls and its tip is the point of connection of the two internal walls. Throughout this article, if not stated otherwise, 'main vessel' means parent main vessel (MV) — MB continuity. The basic parameters of every bifurcation are diameters of parent MV, daughter main and SBs (with smaller than parent vessel diameters) and three angulations: the two proximal between the parent vessel and MB (angle C) and parent vessel — SB (angle B) and third between main and SBs (angle A). Previously, we have also defined carina angle (angle alpha; the complementary angle to angle A we called angle beta), which is actually the smaller distal angle between parent MV and SB [8–11]. This angle governs the extent to which the carina will be displaced from stent struts after stent placement across the SB ostium (for how carina exactly compromises SB ostium, see next paragraph). In general, stent placement in the bifurcation region (even without plaques forming stenosis) will cause a deformation of the whole region — the MV will be straightened with equalisation of proximal and distal MV diameters (MB diameter equals parent vessel diameter — Fig. 1). As a result of this equalisation in proximal and distal MV diameters, and taken together with straightening of MV, there is a deformation at the SB ostium — its internal wall is curved (displaced) to the lateral wall, which occurs simultaneously with the stretching of the SB walls perpendicularly from the plane of bifurcation. All these changes are theoretically predicted according to expected deformation of materials, which can occur if three tubes with different diameters are connected. Our theoretical model (see Appendix 1) describes well how a change in any basic parameter (such as vessel diameters, between vessel angulations), keeping some of the others constant, will cause a change in the remaining parameters (for example how an increase in parent diameters, with constant diameters kept constant, will cause change in between-vessel angulations). These changes will result in changes in carina length and accordingly — SB ostial stenosis, even without any plaque appearance in the bifurcation region. The prediction of this influence is possible, because of the concept of carina length, described in the next paragraph.

Carina length and SB compromise: The carina length is the part of the SB wall facing the MB wall, which is rotated from stent struts laterally and so closing the SB ostium. The fulcrum point of rotation of the carina is a crossing point of lines of the internal SB wall and the lateral parent vessel wall on the side of the SB (Fig. 1C). As demonstrated in Figure 1D, the carina is rotated around its fulcrum point and, depending on its length, it closes ("compromises") the SB ostium.

A useful analogy is to think about the carina and its length as a door closing the ostium of the SB (Fig. 1G). At same doorframe size, the normally sized door closed to some extent (for example at 45 degrees) will close the opening of the doorframe by half. If the door is wider (Fig. 1F) with same door rotation (closure) the doorframe will be closed much more. If the door is much narrower than the normally sized door, at same door rotation/closure the doorframe will be more widely opened (Fig. 1G). We can now think about the carina length as a door closing the SB. In the case of normal opening of SB regarding vessel axis (which occurs generally when the construction of the bifurcation region is governed according to principles of optimal distribution of energy, volume and flow), the carina length is 'optimal' (or 'normal') and it will be displaced to the extent determined from the carina angle (see above) — according to our 'cosine rule' (for further details, see [8]). Non-optimal bifurcation models (bifurcation region constructed not in accordance with optimality principles, see Appendix 1) are assumed to have either a longer or shorter carina length than that of an optimal model. The longer carina length (carina length excess), as with the wider door in our analogy model, can result in more SB ostial stenosis (Fig. 1D); and vice versa — the shorter the carina length (carina length deficit), the less will be the SB closure (compromise). The difference between optimal carina length and actual length was defined as 'carina length mismatch' (see Appendix 2 for further details).

Bench tests

Different types of stents (ML Vision, Abbot Vascular, US; Liberte, Boston Sci. Corp., US; Cypher Select, J&J, US) were implanted in a flexible bifurcation model made by soft polyethylene, which permits wall deformations. The detailed description of a bifurcation model has been given previously [14]. The changes during implantation were observed under microscopy with high grade magnification up to 300 ×.

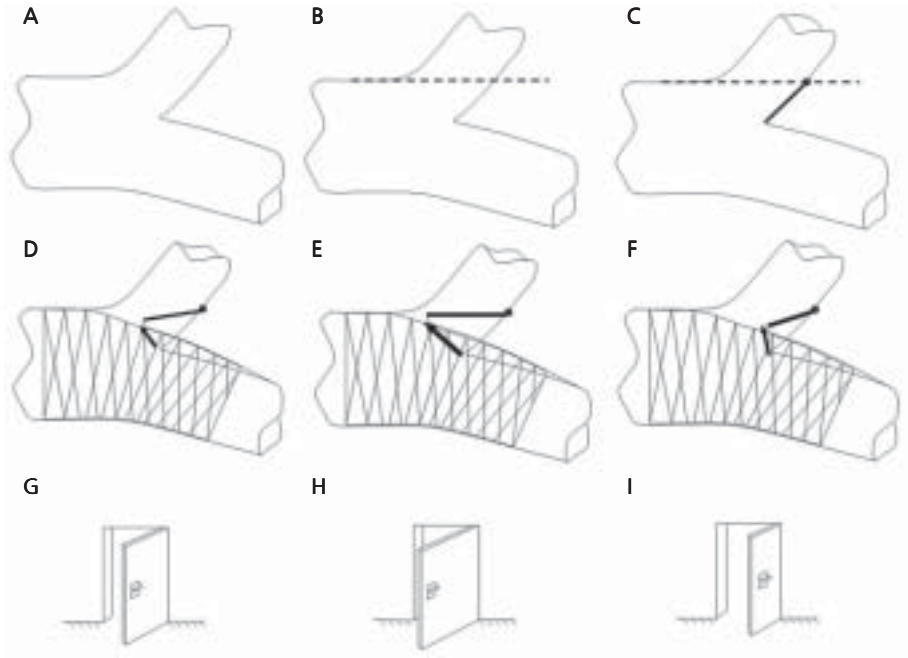

Figure 1. The concept of carina length mismatch and its effect on side branch compromise; **A.** General construction of bifurcation region with approximately normal opening of main branch and side branches according to vessel axes; **B.** The interrupted line traced as continuation of parent vessel lateral wall at side branch side and crossing the internal side branch wall (the wall facing main branch); **C.** The carina length (thicker bold line) with its fulcrum point (the dot with white centre); this is the part of the side branch wall that will be deformed if stent is placed in main vessel; **D.** Influence of different carina lengths on side branch compromise — with increasing the carina length there is larger side branch compromise (2) than with normal length carina, and with decreasing carina length the side branch compromise is less than with normal carina length (3); **E–G.** Cartoon analogy to demonstrate the influence of carina length on side branch compromise; the carina displacement is represented as closing a door (**E**), with wider door (longer carina) closing doorframe more (**F**) and narrower door closing doorframe less (**G**) than normal size door

Study population and prediction of side branch jailing

The patient population consisted of 84 patients with stable or unstable angina with 92 bifurcation lesions treated (Table 1). The inclusion criteria were good quality angiograms permitting good visibility of the carina region, without any vessel wall overlap. The vessels reference size was equal to or more than 3.0 mm for MB, and more than 2.2 mm for SB. The provisional T-stenting was a default strategy with pre- and/or post dilatation of main and SBs, as well as final kissing balloon inflation according to operator decision. 84% had multivessel disease. The left anterior descending artery was the treated vessel in 73% of cases. The SB required treatment in 32 (38%) patients. The length of the carina, carina length mismatch (deficit or excess) was defined according to formula 1 (Appendix 2) and formulas A1–A8 (Appendix 1).

Table 1. Patient demographic characteristics

Age [years]	65 ± 11
Sex — males	56 (67%)
Hypertension	64 (76%)
Dyslipidaemia	69 (82%)
Diabetes	28 (33%)
Smoking	49 (58)
Previous myocardial infarction	26 (31%)
Previous revascularisation	35 (41%)

Angiographic analysis

Quantitative angiographic analyses were performed using commercially available software (Medis QCA version 5.0 and Dicom Works version 3.1.5b). Bifurcation lesions were classified according to the Medina classification [13]. Three bifurcation segments: proximal MB, distal MB, and SB, were analysed separately. Vessel diameter and minimum lumen diameter (MLD) were measured before and after stenting, and percent diameter stenosis (%DS) was calculated. Measurement of carina angles was performed as previously described [4, 5]. The theoretical SB compromise as ostial %DS after stent placement in MV-MB was calculated according to our cosine rule: SB %DS = $\cos\alpha \times 100$ (see details in [8]).

Statistical analysis

All data is presented as means ± 1 SD. Differences between groups were examined with paired or unpaired t-tests as appropriate, with normal distributions. If distribution was not normal, Wilcoxon sign-ranked tests and Mann-Whitney U-tests were performed. Analysis of Variance (ANOVA) was used for multiple comparisons of data, when parameters were distributed normally. Otherwise, a Kruskal-Wallis test was performed. Multiple regression analysis with backward elimination process was used to identify predictors of differences between predicted and observed SB ostial diameter stenosis. All univariate predictors with $p < 0.1$ were included in a multivariate model. χ^2 tests were applied for qualitative data. Significance was determined as p values less than 0.05. All calculations were performed with the SPSS version 13.0 (SPSS Inc., IL, USA).

RESULTS

Bench test results

Three major changes occurred in the geometry of the bifurcation region and MB stent implantation: MV-MB straightening, carina displacement from stent struts, and lateral stretch of SB ostium walls resulting in aggravation of SB ostial stenosis. The last change is caused by a difference in diameters of SB and MV-MB. The SB ostial area became generally elliptical with some irregularities, because of random positioning of stent struts against the SB ostium and the most convex part of the carina. As the changes in the models with all three types of stents were almost identical, representative pictures are given in Figure 2.

Angiographic analysis

The angiographic characteristics relevant to this present analysis are shown in Table 2. After stent implantation in the MV, there was a significant straightening of MV-MB, expressed as a significant increase in angle C and decrease of between branch angle A, mainly because of decrease in angle beta. The MV-SB proximal angle B had almost equal distribution in increasing and decreasing directions, cancelling out each other and giving no change in this angulation. There was a significant correlation between *changes* in angle A and changes in angle B ($r = –0.359$, $p < 0.005$). Moreover, there was a significant correlation between angle B values before stenting and angle B change ($r = –0.389$, $p < 0.001$) — bigger angle B values before stent implantation were associated with largest negative values of angle B change (decrease in MV-SB angle after stent implantation; this decrease is larger with higher initial angle B). There was an excellent correlation between theoretically predicted SB ostial diameter stenosis after stenting according to cosine rule and actually measured ($r = 0.85$, $p < 0.001$). There was a coincidence (within the limits of 3% difference) between predicted and measured %DS in eight (9%) bifurcations. In 35 (38%) lesions, the actually measured SB %DS was larger than expected and in 49 lesions the measured stenosis was smaller than expected (53%). The deviation of SB ostial diameter stenosis from the theoretically predicted values significantly correlated negatively with SB total closure ($n = 5$) and with the rates of diminishing SB flow after stenting ($n = 16$).

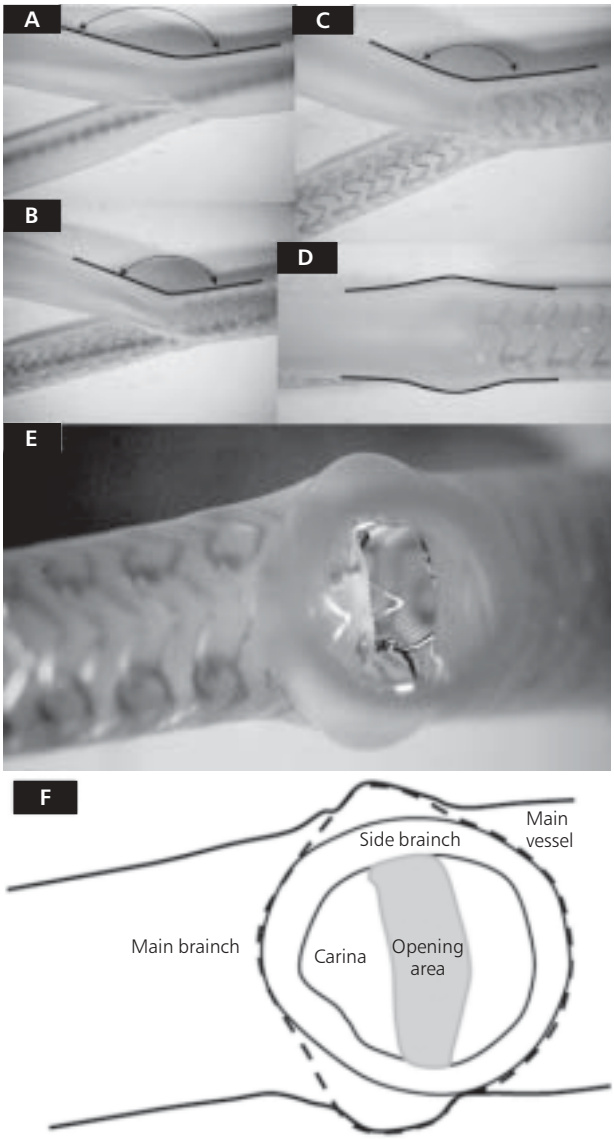

Figure 2. **A.** Model before implantation of Vision stent (Abbot Vascular, US), lateral view; **B.** Stent implantation with decrease of proximal angle between MV and SB and squeesing SB ostium; **C.** After balloon deflation there is small partial restoration of MV-MB angle; **D.** View from above of SB side, there is lateral stretch of SB ostium; **E.** View from SB opening — the carina is displaced from stent struts forming elliptical SB ostial orifice, interrupted lines trace the SB ostium external contour; **F.** Cartoon of SB ostium view (Fig. 2E) with shadowing of SB ostium area; MV — main vessel; SB — side branch; MB — main branch

The difference between theoretically predicted and actual SB %DS after stenting was statistically significantly positively correlated with SB lesion length, positive carina length mismatch (length deficit), and MLD at the SB ostium after stent implantation. There was a significant negative correla-

Table 2. Quantitative angiographic measurements

Angiographic characteristics	Before stent	After stent	P
MV			
MV-RVD [mm]	3.44 ± 0.57	3.48 ± 0.46	NS
MV-MLD [mm]	1.83 ± 0.88	3.12 ± 0.47	< 0.001
MV-%DS	47% ± 24%	6% ± 12%	< 0.001
MV lesion length [mm]	6.55 ± 5.05		
MB			
MB-RVD [mm]	2.91 ± 0.55	3.0 ± 0.47	NS
MB-MLD [mm]	1.35 ± 0.70	2.82 ± 0.47	< 0.001
MB-%DS	54% ± 22%	4% ± 9%	< 0.001
MB lesion length [mm]	9.72 ± 8.21		
SB			
SB-RVD [mm]	2.45 ± 0.45	2.47 ± 0.41	NS
SB-MLD [mm]	1.26 ± 0.55	0.80 ± 0.58	< 0.001
SB-%DS	48% ± 22%	69% ± 19%	< 0.001
Angle A [°]	63 ± 19	61 ± 17	0.047
Angle B [°]	136 ± 20	136 ± 19	NS
Angle C [°]	147 ± 19	156 ± 15	< 0.001
Angle α [°]	41 ± 17	42 ± 16	NS
Angle β [°]	22 ± 13	19 ± 12	0.043
Angle A change [°]		–3 ± 12	
Angle B change [°]		–0.13 ± 11	
Angle C change [°]		10 ± 15	
Angle α change [°]		1 ± 12	
Angle β change [°]		–3 ± 13	

All measures in millimetres unless otherwise stated; MV — main vessel; MB — main branch; SB — side branch; RVD — reference vessel diameter; MLD — minimal lumen diameter; %DS — percentage diameter stenosis; NS — not significant

Table 3. Independent predictors of difference between predicted and observed side branch percentage diameter stenosis after stenting

Predictor	Odds ratio	Confidence interval	P
Carina length mismatch (deficit)	2.568	1.336–4.896	0.003
Main branch reference vessel diameter	0.314	0.101–0.972	0.02
Angle B change	0.926	0.870–0.985	0.039

tion with MB reference diameter, angles A, B and alpha, angle B change, main branch MLD before and after stenting, stent diameter and implantation pressure, and MB final MLD. Independent associates of difference between theoretically predicted and observed SB %DS on multivariate analysis are presented in Table 3.

A plot comparing the values of carina length mismatch and deviations from the prediction in SB ostial percentage diameter stenosis is shown in Figure 3. Depending on the combination between those two parameters, three zones are formed: zone I with smaller than expected SB compromise and shorter carinas, 54% from total population (n = 50); zone II with higher than expected SB compromise and shorter carina length, 30% (n = 27); and zone III with higher SB compromise and longer carina length, 13% (n = 12). The other three bifurcation lesions did not fit in any category. The independent predictors from multiple logistic regression analysis of the difference between the observed and the actual SB ostial percentage diameter stenosis after stenting are presented in Table 3.

DISCUSSION

Significant ostial SB stenosis after MV-MB stent placement could cause persistent ischaemia and symptoms. The exact mechanisms of this phenomenon are not completely clear. Recently, we proposed that carina displacement from the stent struts in the main vessel is the main mechanism causing significant ostial narrowing of the SB [9–11, 13] and proposed a quantitative rule to predict the extent of this stenosis [8]. Previously we demonstrated that deviations from theoretically predicted SB compromise could be related to outcome, and we concentrated in the present article on analysis of factors responsible for these deviations [9, 13].

The additional aim of this study was to give a theoretical basis for differing effects of carina region deformation (carina

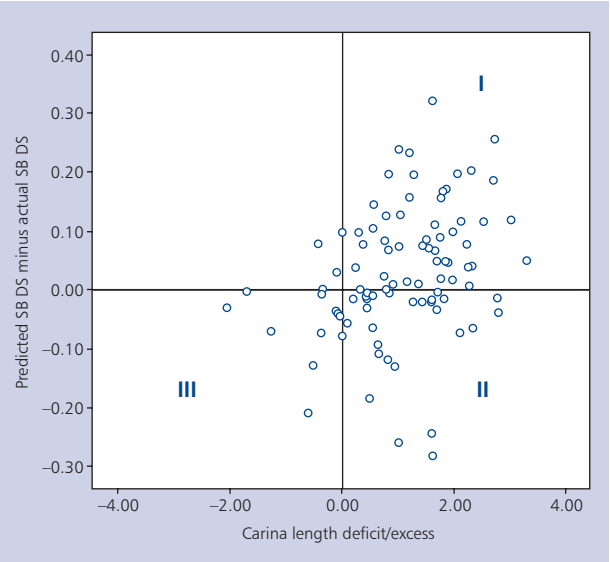

Figure 3. Comparison of carina length mismatch (carina length excess or deficit calculated according to formula 3 in Appendix 2 with difference between predicted and observed SB %DS after main vessel stenting. I — zone with less than expected SB %DS and carina length deficit; II — zone with larger than expected SB %DS and carina length deficit; III — zone with larger than expected SB %DS and carina length excess. The carina length mismatch (deficit/excess) as difference in lengths is expressed in millimetres. SB %DS is expressed in decimal units (0.1 = 10%); SB — side branch; DS — diameter stenosis

displacement, lateral SB stretch with proximal wall flexion) from the plaque shift as factors of SB jailing in coronary bifurcation lesions. We focused on the role of carina length mismatch on the deviations of measured SB stenosis from theoretically predicted stenosis. Carina length mismatch was defined as deficit if calculated length is shorter than theoretically expected for a given bifurcation parameters, or as excess if carina is longer. In a plot comparing the values of carina length mismatch and deviations from the prediction in SB ostial stenosis, most cases were located in three zones. The first one (zone I in Fig. 3) is cases with shorter carina lengths and smaller than expected SB ostial stenosis. In these cases, carina displacement seems to be a leading mechanism of SB compromise and occurred in 54% of cases. Zone II reflects the situation with shorter carina and more SB compromise than expected. The mechanisms of SB jailing in these patients seem to be both plaque and carina shifting and occurs in 30% of cases. Cases with longer carina and more SB jailing than expected were located in zone III. It is possible that in this situation again, carina displacement could be a leading mechanism of SB compromise.

From these results, it is highly probable that carina deformation is the responsible mechanism for SB jailing in almost two thirds of cases, but that plaque shift also can play a considerable role in other patients.

Limitations of the study

The main limitations of our study are its small sample size, possible selection bias, and lack of validated software for bifurcation lesion evaluation and especially for angulation measurement. In the present study, attempts were made to standardise the method used for angle measurement. However, there is still the potential for variability due to the variability in geometry during the cardiac cycle, and the variability due to small changes in angulation of the camera gantry. The obvious limitation of our elastic bifurcation model is lack of plaque as well as homogeneity of wall components. Theoretically different wall components as well as their different distributions in vessel walls will influence wall deformation, even if the wall has homogenous thickness. The situation became even more complex if there was difference in wall thickness, especially if it was distributed unequally. Our model does not incorporate these factors. It is possible that with increasing accuracy of multislice computed tomography, it will become possible to explore the influence of all the above mentioned factors on SB compromise.

CONCLUSIONS

After main vessel stent placement in a coronary bifurcation lesion, a complex change in this region occurs and results in SB jailing. The degree of SB jailing seems to be determined by the carina deformation, the length of the carina, and plaque shift.

Conflict of interest: *none declared*

References

1. Iakovou I, Schmidt T, Bonizzoni E et al. Incidence, predictors, and outcome of thrombosis after successful implantation of drug-eluting stents. JAMA, 2005; 293: 2126–2130.
2. Latib A, Colombo A. Bifurcation disease: what do we know, what should we do? J Am Coll Cardiol Cardiovasc Interv, 2008; 1: 218–226.
3. Mayor M, Malik AZ, Minor RJ Jr et al. One-year outcomes from the TAXUS express stent versus cypher stent. Am J Cardiol, 2009; 103: 930–936.
4. Niccoli G, Ferrante G, Porto I et al. Coronary bifurcation lesions: To stent one branch or both? A meta-analysis of patients treated with drug eluting stents. Int J Cardiol, 2008 [Epub ahead of print].
5. Stankovic G, Darremont O, Ferenc M et al.; European Bifurcation Club. Percutaneous coronary intervention for bifurcation lesions: 2008 consensus document from the fourth meeting of the European Bifurcation Club. EuroIntervention, 2009; 5: 39–49.
6. Zhang F, Dong L, Ge J. Simple versus complex stenting strategy for coronary artery bifurcation lesions in the drug-eluting stent era: a meta-analysis of randomized trials. Heart, 2009; 95: 1676–1681.
7. Michalek A, Vassilev D, Walecki J et al. Does periprocedural myonecrosis after main vessel stenting of coronary bifurcations occur? Assessment by means of MRI delayed enhancement. Am J Cardiol, 2009; 104: 41D–42D.
8. Vassilev D, Gil RJ. Relative dependence of diameters of branches in coronary bifurcations after stent implantation in main vessel: importance of carina position. Kardiol Pol, 2008; 66: 371–378.
9. Vassilev D, Gil R. Clinical verification of a theory for predicting side branch stenosis after main vessel stenting in coronary bifurcation lesions. J Interv Cardiol, 2008; 21: 493–503.
10. Vassilev D, Gil RJ. Changes in coronary bifurcations after stent placement in the main vessel and balloon opening of stent cells: theory and practical verification on a bench-test model. J Geriatr Cardiol, 2008; 5: 43–49.
11. Vassilev D, Gil RJ, Rzezak J et al. Determinants of side branch compromise after main branch stent implantation in coronary bifurcation lesions: application of quantitative rule. Am J Card, 2008; 101: S38.
12. Koo BK, Waseda K, Kang HJ et al. Anatomic and functional evaluation of bifurcation lesions undergoing percutaneous coronary intervention. Circ Cardiovasc Interv, 2010; 3: 113–119.
13. Gil RJ, Vassilev D, Formuszewicz R et al. The carina angle-new geometrical parameter associated with periprocedural side branch compromise and the long-term results in coronary bifurcation lesions with main vessel stenting only. J Interv Cardiol, 2009; 22: E1–E10.
14. Vassilev D., Gil RJ. Changes in coronary bifurcations after stent placement in the main vessel and balloon opening of stent cells: theory and practical verification on a bench-test model. J Geriatr. Cardiol, 2008; 5: 43–49.
15. Zamir M. Optimality principles in arterial branching. J Theor Biol, 1976; 62: 227–251.

APPENDIX 1. DESCRIPTION OF THE BIFURCATION CONFLUENCE REGION

Let us assume that the bifurcation region is formed from crossing of three axes of the parent vessel and two daughter vessels — MB and SB. The crossing point of the three axes will be called the bifurcation confluence point (Fig. A1). The requirements of our model are that the diameters of all vessels are normal to vessels' axes and the branch vessels start to diverge from the main vessel simultaneously, thus ensuring blood entry to those vessels at the same moment. This is a reasonable assumption, because the flow must be laminar and this ensures the fastest and shortest way of fluid transportation from one site to another within the vascular system. The point of confluence of all vessel axes forming the bifurcation is located at the carina tip — the place of MB and SB facing walls connection (Fig. A2). It is not required that midlines of SB and MB cross in one point. The branch vessels make angles with parent vessel axis — we will call it α for SB and β for MB. If the diameters of the MB (d_m) and SB (d_s) vessels are given, together with values of angles α and β, the parent vessel diameter (d_p) could vary between d_{p0} and $d_{p\text{-}max}$ (double arrow in Fig. A3). These two extreme values for parent vessel diameters are physiologically irrelevant, as great pressure gradients are required to maintain adequate flow in the branch vessels. Thus, the actual diameter of the parent vessel, d_p, dependson distance h_a, i.e. the distance from d_{p0} (Fig. A2).

It was assumed that the total bifurcation construction will be governed by some optimality principles. Our model gives a general description of bifurcation construction and mathematical apparatus for describing changes occurring if some parameters are met. There are two important internal parameters of the bifurcation — the carina position, dividing and distributing the flow in branch vessels, which could be expressed as the value of parameter c_s (SB flow distance); and the length of zone of flow change from parent to branch vessels, h (changing flow length). It is important to note that varying the position of the parent vessel's opening to the branch vessels varies not only its diameter, but also the carina position and so — the relative amount of flow entering each vessel.

From the trigonometry we have the following relations:

$$d_{po} = [(d_m/\sin\beta) - (d_s/\sin\alpha)] \times \operatorname{tg}\beta + c_m + c_s \quad \text{(A1)}$$

$$c_s = h_a \times \operatorname{tg}\alpha \quad \text{(A2)}$$

$$c_m = h_a \times \operatorname{tg}\beta \quad \text{(A3)}$$

Based on equations A1–A3 we find the expression for c_s, h_a and h:

$$h_a = \{d_p \times \sin\alpha \times \cos\beta - d_m \times \sin\alpha + d_s \times \sin\beta\}/\{\sin(\alpha+\beta) \times \operatorname{tg}\alpha\} \quad \text{(A4)}$$

$$c_s = \{d_p \times \sin\alpha \times \cos\beta - d_m \times \sin\alpha + d_s \times \sin\beta\}/\{\sin(\alpha+\beta)\} \quad \text{(A5)}$$

$$h = \{d_m \times \cos\alpha + d_s \times \cos\beta - d_p \times \cos\alpha \times \cos\beta\}/\{\sin(\alpha+\beta)\} \quad \text{(A6)}$$

The relative position of the carina is determined from the ratio $C = c_s/(c_m + d_{po})$, as well as the relative position of parent vessel opening at the branch divergence point by the ratio $H = h_a/h$. The branch vessels' openings (double arrows on Fig. A2) have ellipsoid shapes with shorter diameters equal to branch reference diameter and long axis diameters:

$$d_{mo} = \sqrt{[(c_m + d_{po})^2 + h^2]} \quad \text{(A7)}$$

$$d_{so} = \sqrt{[c_s^2 + h^2]} \quad \text{(A8)}$$

In case of bifurcation construction according to minimum surface area at the point of confluence the SB and MB opening diameters coincide with vessel reference diameters.

Thus the group of equations A5–A8 fully describes all parameters of zone of connection of three vessels forming bifurcation. This model permits a complete description of changes in the confluence region if some of parameters, diameters or angles, i.e. the accommodation of bifurcation.

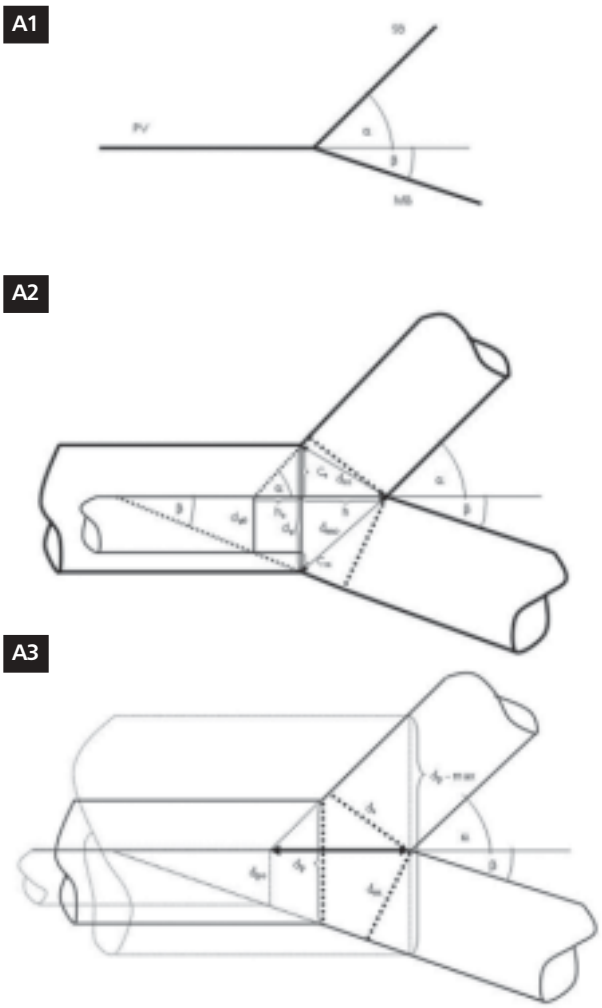

Appendix Figure A1 (shortcuts are in the text). **A1.** Three lines forming carina tip, which are internal walls of daughter branches crossing the parent vessel axis going through the carina tip; **A2.** The actual bifurcation confluent region construction; the boundary case with minimal parent vessel diameter d_{p0} is also shown; **A3.** The boundary cases of minimal (d_{p0}) and maximal (d_p – max) parent vessel diameters are shown.

APPENDIX 2. CARINA LENGTH MISMATCH CONCEPT

We assume that after main vessel stenting there are several changes occurring in the bifurcation confluence region. Firstly, there is straightening of the MV-MB connection. Secondly, the carina is displaced to the SB direction. This change is accompanied by lateral stretch of the side branch walls in a direction perpendicular to the MV-MB axis. The last deformation causes elliptical formation of the SB ostium, giving larger ostial area than assumed based only on a circular assumption of the SB ostium. This deformation, in combination with the previous two, leads to a decrease of MV-SB proximal angle [10]. We propose the term 'carina region deformation' to summarise the description of all these changes, as they occur simultaneously. The most important of these changes with regard to SB compromise is the carina displacement determining the extent of SB ostial stenosis after main vessel stenting. We previously have shown that by estimating (measuring from angiography) the distal MV-SB angle, called the carina angle alpha (a), it is possible to predict, with a great degree of confidence, the extent of percentage diameter ostial stenosis of a SB according to the simple equation SB %DS = cos α × 100, where SB %DS is a side branch ostial percentage diameter stenosis [12, 13]. It must be stressed that this prediction is based on the assumption that the bifurcation confluence region is constructed according to the optimality principle of optimising minimal surface area. However, as is evident from the work of Dr. Mair Zamir [15], the bifurcation confluence region could be constructed according to different optimality principles, thus giving different constructions of the confluence region with identical entry parameters. This means that even if the bifurcation is optimally constructed according to some optimality principle, it could have a different type of appearance of bifurcation confluence region according to another optimality principle. The different construction of this region will influence to a different extent carina region deformation and SB compromise.

The carina region deformation is influenced by the different construction of the confluent region through the different carina lengths. The carina length is the distance between the carina tip and the intersection point of MV outer wall tangent line and tangent line of SB internal wall (facing MB, see Appendix Fig. 2). This is the part of the SB wall which is rotated because of the stent implantation and which occludes the branch ostium. It is obvious that its length will influence the extent to which the SB ostium is 'closed' — shorter carina length causes less SB compromise, while longer carinas will cause more SB compromise compared to the situation with optimal configuration (Fig. 1).

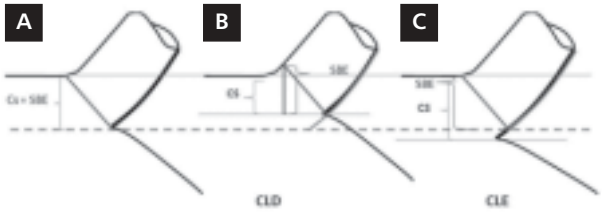

Appendix Figure 2. The carina length mismatch concept — the figure presents side branch (SB) position from the bifurcation confluence region. The carina length is the distance between the carina tip and intersection point between tangent lines of outer main vessel wall and side branch internal wall, facing MB; **A.** Ideal construction, when SB opening is equal to the branch reference diameter; SBE — side branch extension distance is the distance occupied from the SB ostium from parent vessel diameter, here equal to cs — side branch flow distance, as defined in Appendix 1; **B.** Carina length deficit (CLD) — the actual carina is shorter than optimal; cs < SBE; **C.** Carina length excess (CLE) — the carina is longer than optimal; cs > SBE.

The length of the carina (l) in an actual situation (a) and in optimal conditions (o) could be calculated according to the following formulas:

$$l_a = cs/\sin \alpha \quad (1)$$

$$l_o = ds \times \cos \alpha/\sin \alpha \quad (2)$$

The difference between the two lengths is a mismatch length:

$$M = ds \cot an \alpha - cs \times cosec \alpha \quad (3),$$

where M — carina length mismatch (deficit or excess), ds — SB reference diameter, alpha angle is defined as above, cotan α — cotangent alpha, cosec α — cosecant alpha. The cs is SB flow distance — the distance between two lines: parallel line of lateral MV wall from SB side passing through carina tip and lateral MV wall per se (Fig. 1).

If M > 0, then there is carina length deficit, if M < 0, then carina length excess is observed (Appendix Fig. 2). All required parameters in the formula could be measured from coronary angiography.

Parametry wpływające na zwężenie bocznej gałęzi po stentowaniu głównego naczynia w leczeniu zmian obejmujących rozwidlenie tętnicy wieńcowej

Dobrin Vassilev[1], Robert J. Gil[2, 3], Bon-Kwon Koo[4], C. Michael Gibson[5], Thach Nguyen[6], Thai Hoang[7], Nina Gotcheva[8]

[1]Cardiac Catheterisation Laboratory, National Heart Hospital, Sofia, Bułgaria
[2]Klinika Kardiologii Inwazyjnej, Centralny Szpital Kliniczny Ministerstwa Spraw Wewnętrznych i Administracji, Warszawa
[3]Instytut Medycyny Doświadczalnej i Klinicznej, Polska Akademia Nauk, Warszawa
[4]Seoul National University Hospital, Korea Południowa
[5]Cardiovascular Division, Beth Israel Deaconess Medical Center, Harvard Medical School, Boston, MA, Stany Zjednoczone
[6]St. Mary Medical Center, 1500 South Lakepark Ave, Hobart, IN, Stany Zjednoczone
[7]University of Arizona, Sarver Heart Center, Southern Arizona VA Health Care System, Tucson, AZ, Stany Zjednoczone
[8]National Heart Hospital, Sofia, Bułgaria

Streszczenie

Wstęp i cel: Niniejszą analizę przeprowadzono w celu określenia czynników przyczyniających się do rozwoju zwężenia bocznej gałęzi po stentowaniu głównego naczynia.

Metody: Stworzono teoretyczny i praktyczny model rozwidlenia z różną długością ostrogi. W celu obserwacji zmian okolicy rozwidlenia po implantacji stentu przeprowadzono praktyczne eksperymenty ze zmiennym modelem rozwidlenia. Wykonano również angiograficzną analizę 92 zmian obejmujących rozwidlenie (u 84 pacjentów) w celu określania wpływu teoretycznych parametrów na zwężenie bocznej gałęzi w praktyce. U tych osób porównano teoretycznie przewidywane i faktycznie obserwowane zwężenie bocznej gałęzi.

Wyniki: Praktyczne eksperymenty wykazały złożone zmiany w okolicy rozwidlenia w zależności od przemieszczenia ostrogi, rozciągnięcia ścian bocznej gałęzi i zmniejszenia proksymalnego kąta między głównym naczyniem a boczną gałęzią po wprowadzeniu stentu do głównego naczynia. W analizie angiograficznej faktycznie zmierzony stopień zwężenia światła bocznej gałęzi był większy od przewidywanego w 35 (38%) zmianach, natomiast mniejszy od przewidywanego w 49 zmianach. Do niezależnych wskaźników predykcyjnych różnicy między teoretycznie przewidywanym a obserwowanym stopniem zwężenia bocznej gałęzi należały: niedopasowanie długości ostrogi [iloraz szans (OR) 2,568, przedział ufności (CI) 1,336–4,896), referencyjna średnica głównej gałęzi (OR 0,314, CI 0,101–0,972) oraz zmiana proksymalnego kąta między głównym naczyniem a boczną gałęzią po stentowaniu (OR 0,926, CI 0,870–0,985). Na wykresie porównującym wartości niedopasowania długości ostrogi z odchyleniem od przewidywanego stopnia ostialnego zwężenia bocznej gałęzi 27 (30%) przypadków znajdowało się w strefie krótszej odnogi i większego stopnia zwężenia bocznej gałęzi niż przewidywano, co wskazuje na rolę przesunięcia blaszki miażdżycowej w tych przypadkach.

Wnioski: Wydaje się, że stopień zwężenia bocznej gałęzi zależy od deformacji ostrogi, jej długości, a także przesunięcia blaszki miażdżycowej.

Słowa kluczowe: stentowanie rozwidlenia tętnicy wieńcowej, deformacja ostrogi, długość ostrogi, przesunięcie blaszki miażdżycowej

Kardiol Pol 2012; 70, 10: 989–997

Adres do korespondencji:
Dobrin Vassilev, MD, PhD, Cardiac Catheterisation Laboratory, National Heart Hospital, Sofia, Bulgaria, 65 Koniovitza Str., 1309 Sofia, Bulgaria, e-mail: dobrinv@gmail.com
Praca wpłynęła: 01.02.2012 r. **Zaakceptowana do druku:** 09.05.2012 r.